Inorganic Chemistry

Article

pubs.acs.org/IC

Flexibility is Key: Synthesis of a Tripyridylamine (TPA) Congener with a Phosphorus Apical Donor and Coordination to Cobalt(II)

Zachary Thammavongsy, Juliet F. Khosrowabadi Kotyk, Charlene Tsay, and Jenny Y. Yang*

Department of Chemistry, University of California, Irvine, California 92697, United States

Supporting Information

ABSTRACT: Tripyridylamine (TPA), a tetradentate ligand that forms 5-membered chelate rings upon metal coordination, has demonstrated significant utility in synthetic inorganic chemistry. An analogue with a phosphorus apical donor is a desirable target for tuning electronic structure and enhancing reactivity. However, this congener has been synthetically elusive. Prior attempts have resulted in tridentate coordination to transition metal ions due to a lack of ligand flexibility. Herein, we report the successful synthesis of tris(2-pyridylmethyl)proazaphosphatrane (TPAP), a more accommodating tripyridyl ligand containing an apical phosphorus donor. The TPAP ligand forms 6-membered chelate rings upon coordination and binds in the desired tetradentate fashion to a Co(II) ion. Structural studies elucidate the importance of ligand flexibility in tripodal ligands featuring phosphorus donors. Cyclic voltammetry, UV−vis, and solution magnetic susceptibility experiments of $[Co(TPAP)(CH_3CN)]^{2+}$ are also reported and compared to $[Co(TPA)(CH_3CN)]^{2+}$. Notably, magnetic susceptibility measurements of $[Co(TPAP)(CH_3CN)]^{2+}$ indicate a low spin electronic configuration, in contrast to $[Co(TPA)(CH_3CN)]^{2+}$, which is high spin.

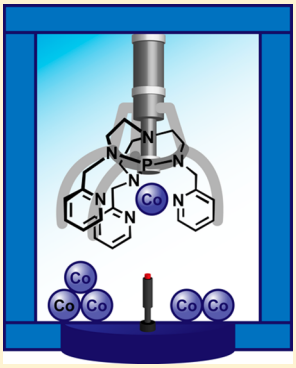

INTRODUCTION

Complexes containing neutral tetradentate tripodal ligands[1] are widely used in coordination chemistry for a variety of catalytic applications including oxygen reduction,[2] hydroxylation,[3] epoxidation,[4] aziridination,[5] and atom-transfer radical polymerization.[6] These complexes have also been extensively used to model enzymatic active-sites.[7] Additionally, transition metal complexes in this coordination environment are known to exhibit interesting electronic properties such as spin-crossover behavior.[8] The most widely studied ligands of this type are neutral tripyridyl ligands containing an apical nitrogen donor, such as tris(2-pyridylmethly)amine (TPA) and, to a lesser extent, tris[2-(2-pyridyl)ethyl]amine (TEPA), shown in Chart 1.

For TPA and TEPA, tetradentate chelation is predominately observed, where the ligands form 5- and 6-membered chelate rings, respectively, with the metal ion. This leaves an open coordination site for substrate binding trans to the apical nitrogen donor. As a result, replacing the apical nitrogen donor has been the most effective way to tune substrate activation. For example, the nitrogen in TPA has been replaced with analogues containing carbon,[9] silicon,[10] and tin[11] to modulate the reactivity of the corresponding metal complexes. Substituting the apical nitrogen with a phosphorus donor, which is a stronger π-acid, has been predicted to expand the scope of reactivity, particularly with substrates capable of π interaction with the metal, such as dinitrogen and dioxygen.[12−15]

However, a TPA congener with a phosphorus apical donor has been synthetically elusive. Chiswell reported the synthesis of a tripyridyl ligand with a central phosphine donor (tri(pyridylmethyl)phosphine (TPPh), Chart 1) in 1967, but did not structurally characterize the corresponding Mn(II), Ni(II), and Co(II) complexes.[16] More recently, Britovsek et al. reported the synthesis of tri(*N*-methyl-pyridylamino)phosphine (TPAMP) and an improved preparation for TPPh as potential TPA analogues.[17] Structural analysis by X-ray crystallography of the corresponding Cr(III), Fe(II), and Ru(II) complexes for both TPPh and TPAMP revealed tridentate coordination with the phosphorus donor and two pyridine ligands.[17] Britovsek

Chart 1. Neutral Tripodal Tripyridyl Ligands with N and P Apical Donors[a]

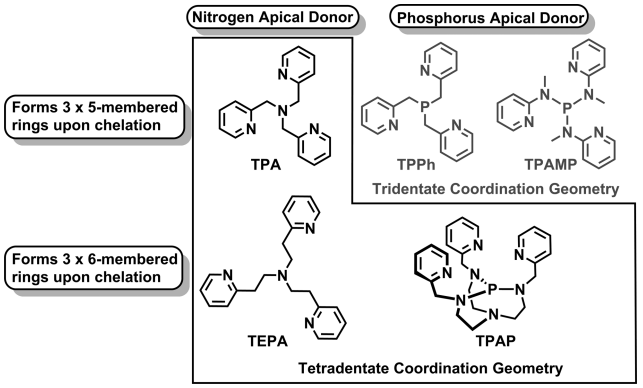

[a]The ligands coordinate to form either 5- (TPA, TPPh, and TPAMP, top row), or 6- (TEPA and TPAP, bottom row) membered chelate rings with the metal.

Received: September 16, 2015
Published: November 9, 2015

DOI: 10.1021/acs.inorgchem.5b02133
Inorg. Chem. 2015, 54, 11505−11510

and co-workers attributed the absence of tetradentate chelation for TPPh and TPAMP to longer M—P bond distances compared to the M—N distance in TPA complexes, concluding that this "allow[s] only two pyridyl units to comfortably coordinate to the metal center."[17]

In contrast, Ballmann et al. reported tris(3-aminopropyl)-phosphine (TRPN), with three anionic nitrogen ligands and an apical phosphorus donor, which coordinates to group 4 metal ions in a tetradentate fashion.[18] Ballmann and co-workers hypothesized that the coordination behavior of anionic $[PN_3]$ ligands is dependent on the length of the N—C_n—P linkage (n = 1–3).[19] They concluded that a 3-atom linker would provide sufficient flexibility for all four donor atoms to chelate, forming 6-membered chelate rings. Although their work is based on trianionic $[PN_3]$ ligands, we applied their hypothesis regarding linker length to neutral $[PN_3]$ ligand systems in order to successfully synthesize a tetradentate phosphine derivative of TPA.

Herein, we present the synthesis of a new tripyridyl ligand with a phosphorus donor that coordinates in the desired tetradentate fashion to a Co(II) ion. Preparation of this ligand, tris(2-pyridylmethyl)proazaphosphatrane (TPAP) (Chart 1), begins by modifying a proazaphosphatrane colloquially known as Verkade's superbase.[20] The modular synthesis of Verkade's superbase permits facile incorporation of three pyridyl ligands above the proazaphosphatrane base,[21] which forms 6-membered chelate rings upon metal coordination.

RESULTS AND DISCUSSION

Synthesis and Characterization of TPAP. Synthesis of the new TPAP ligand is shown in Scheme 1. The precursor,

Scheme 1. Synthesis of Tris(2-pyridylmethyl)proazaphosphatrane

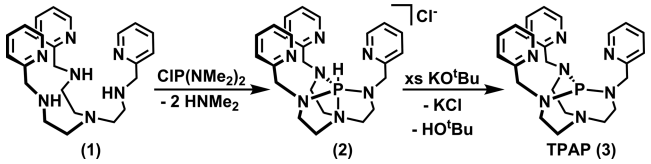

tris[2-[*N*-(2-pyridinemethyl)-amino]ethyl]amine (**1**), was prepared as previously described.[22] Schiff-base condensation of 3 equiv of picolinaldehyde with tris(2-aminoethyl)amine followed by hydrogenation gave **1** as a dark orange oil in 84.3% yield. The addition of bis(dimethylamino)chlorophosphine to **1** yielded the protonated ligand [HTPAP][Cl] (**2**) along with dimethylamine. The latter can easily be removed by washing with tetrahydrofuran, and drying the resulting solid under reduced pressure overnight furnishes **2** as a white solid in 61.9% yield (^{1}H NMR and ^{13}C{^{1}H} NMR shown in Figures S1 and S2, respectively). The ^{31}P{^{1}H} NMR spectrum of **2** features a singlet at −10.0 ppm, which appears as a doublet in the ^{31}P NMR with a *J*-coupling of 506 Hz, consistent with a protonated phosphine (Figure S3 and S4).[23]

Single crystals suitable for X-ray analysis were grown by layering diethyl ether over a solution of **2** in acetonitrile. The solid-state structure of compound **2** displayed a P—N1 distance of 1.971(16) Å and a P—H distance of 1.24(2) Å (Figure 1). These bond distances are similar to previously reported variations of protonated Verkade's superbase.[23−25] The significant Brönsted basicity of Verkade's superbase (pK_a of protonated superbase = 32.9 in CH_3CN)[26] is attributed to

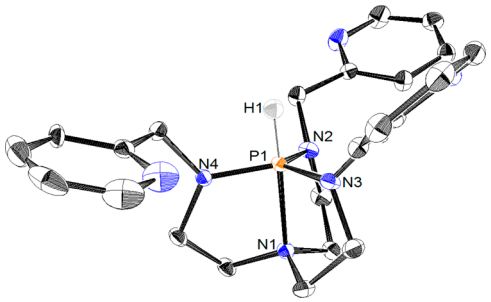

Figure 1. Crystal structure of **2**. Thermal ellipsoids drawn at 50% probability; hydrogen atoms and chloride anion were omitted for clarity except for H1, which was located in the difference map and refined freely.

electron donation from the trans nitrogen atom (N_{trans}, or N1 in structure of **2**) to the phosphorus, which stabilizes the protonated form. This strong interaction between the P and N_{trans} has been observed in prior structural characterization of protonated versus nonprotonated bases.[27] When protonated, the P—N_{trans} distances are typically 2.0 Å or less, while the corresponding free bases have P—N_{trans} distances of over 3.0 Å (see Table S1 for compiled structural data).

Deprotonation of **2** with excess potassium *tert*-butoxide in tetrahydrofuran furnishes TPAP (**3**) as a white solid in 85.4% yield. Ligand **3** was characterized by ^{1}H and ^{13}C{^{1}H} NMR spectroscopy (shown in Figures S5 and S6, respectively). Additionally, the ^{31}P NMR spectrum of **3** exhibits a singlet at 126 ppm (Figure S7), consistent with complete deprotonation.

Synthesis and Structural Studies of Cobalt Complexes. To examine the relationship between linker length and tetradentate coordination in tripyridyl ligands with an apical phosphorus donor, we also prepared the Co(II) complex of the previously reported TPAMP ligand (**4** in Chart 2).[17] TPAMP

Chart 2. Co(II) Complexes

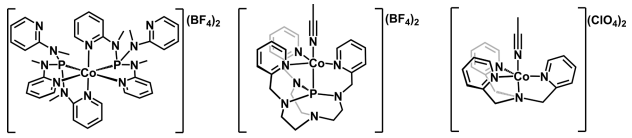

lacks the methylene linker between the phosphorus donor and the pyridine ligand. As a result, coordination of the pyridine linker and the phosphorus donor forms 5-membered chelate rings. One equivalent of TPAMP in dichloromethane was combined with one equivalent of $[Co(CH_3CN)_6][BF_4]_2$ in acetonitrile. Electrospray ionization mass spectrum (ESI-MS) of the reaction mixture reveals the presence of the $[Co(TPAMP)_2]^{2+}$ ion and an absence of the $[Co(TPAMP)]^{2+}$ ion. The isolated product $[Co(TPAMP)_2][BF_4]_2$ (**4**) was precipitated and washed with diethyl ether to afford a green solid in 32.5% yield. Complex **4** was analyzed by single crystal X-ray diffraction (Figure 2). Selected bond distances and angles are shown in Table 1. The crystal structure shows two 6-coordinate $[Co(TPAMP)_2]^{2+}$ complexes in the asymmetric unit. In each TPAMP ligand, only two pyridines and the central phosphorus donor are coordinated, leaving one pyridine unbound to the Co(II) center. This is similar to the binding mode previously observed with Cr(III), Fe(II), and Ru(II).[17]

DOI: 10.1021/acs.inorgchem.5b02133
Inorg. Chem. 2015, 54, 11505−11510

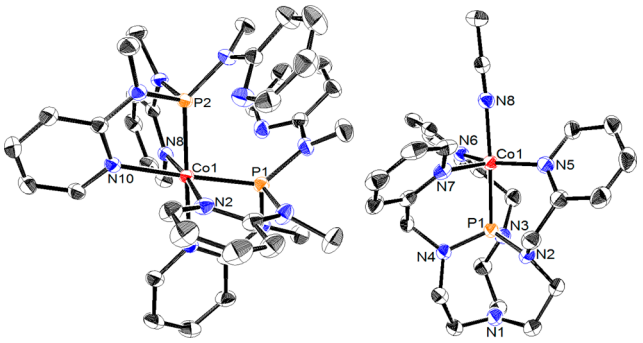

Figure 2. Crystal structure of (left) one of two $[Co(TPAMP)_2][BF_4]_2$ (**4**) molecules in the asymmetric unit and (right) $[Co(TPAP)(CH_3CN)][BF_4]_2$ (**5**). Thermal ellipsoids drawn at 50% probability; hydrogen atoms and BF_4^- anions omitted for clarity.

$[Co(TPAP)(CH_3CN)][BF_4]_2$ (**5**) was prepared by reacting stoichiometric quantities of TPAP (**3**) with $[Co(CH_3CN)_6][BF_4]_2$ in acetonitrile. The product was precipitated and washed with diethyl ether to give the analytically pure product in 56.2% yield. The formulation was confirmed by ESI-MS. A single crystal for X-ray analysis was grown by layering pentane over a solution of **5** in dichloromethane. The structure is shown in Figure 2, and selected bond distances and angles are shown in Table 1. The Co—N_{pyr} distance is similar for all three pyridines (1.997(2), 2.035(2), and 2.094(2) Å), and the Co—P distance is 2.1693(7) Å. The ligand chelates in the desired tetradentate fashion, with an acetonitrile solvent taking up a fifth coordination site. The pseudosquare pyramidal cobalt center has a τ_5 parameter of 0.4176, where a value of 0 represents an ideal square pyramid, and a value of 1 represents an ideal trigonal bipyramid.[28]

In terms of linker length, TPAP is a closer analogue to the amine donor TEPA. However, only two structurally characterized examples of cobalt complexed to TEPA were found in the Cambridge Crystallographic Database Centre (CCDC) (Table S3). In both cases, the cobalt was in the 3+ oxidation state and formed 6-coordinate complexes with bidentate CO_3^{2-} or HCO_3^- anions. As a result, we compared the crystallographic structure of $[Co(TPAP)(CH_3CN)][BF_4]_2$ (**5**) to the structure of the previously reported $[Co(TPA)(CH_3CN)][ClO_4]_2$ (**6**).[29] The distances of Co—N_{pyr} in **6** are 2.037(3), 2.041(3), and 2.053(3) Å for an average distance of 2.044 Å, comparable to the 2.042 Å distance in **5**. The Co—N_{apical} distance of **6** is 2.177 Å, which is also close to the Co—P_{apical} distance of 2.169 Å in **5**. However, **6** has a τ_5 value of 0.99, a geometry much closer to trigonal bipyramidal compared to the pseudosquare pyramidal geometry of **5**. This appears to be a general trend among structurally characterized 5-coordinate $[Co(TPA)(X)]^{2+}$ ions. Twenty-four structures of this type are reported in the CCDC, and all but 1 are closer to a trigonal bipyramidal coordination geometry ($\tau_5 > 0.5$). A complete list of reported structures and analysis is available in the SI. The TPAP and TPA ligands in **5** and **6** contain apical donors close to tetrahedral geometry. The average angle between the Co(II), apical donor, and N or C bound to the apical donor is 109.9° and 106.6° for **5** and **6**, respectively. In contrast, the two pyridines bound to Co(II) in **4** exhibit an average Co—P_{apical}—N angle of 104.5°. The smaller angle found in TPAMP is likely the source of the steric strain that prevents the third pyridine from coordinating to the metal.

In the three structurally characterized examples of Verkade's superbase coordinated to the metal ions Pt(II),[30] Re(I),[31] and Hg(II),[31] the P—N_{trans} distances are all around 3.0 Å, indicating little or no interaction between the phosphorus and N_{trans}. This is consistent with the P—N_{trans} distance of 2.877(2) Å observed in $[Co(TPAP)(CH_3CN)][BF_4]_2$ (**5**). However, these examples all involve coordination to electron rich metal centers. It is possible that N_{trans} can serve as an electron donor to the P and stabilize electron deficient metal centers, similar to the protonated ligand. We are currently exploring this feature of TPAP.

Magnetic Susceptibility. The magnetic moment of six-coordinate **4**, measured by the Evans method in CD_3CN, was 2.11 μ_B, consistent with an S = 1/2 spin state. This is due to the strong ligand donation of both TPAMP ligands in an octahedral coordination geometry around Co(II).

The solution μ_{eff} of **5** was also measured by the Evans method in CD_3CN to yield a magnetic moment of 2.67 μ_B, corresponding to an S = 1/2 system (Figure S8). This is consistent with other cobalt complexes containing strong ligand donors.[32,33] Additionally, perpendicular (⊥)-mode EPR spectroscopy was performed on **5** in acetonitrile at 77 K (Figure 3). The signal for **5** was centered at g = 2.18, corroborating the spin state observed at room temperature using Evans method.

In contrast, TPA is a weak ligand donor; the solution magnetic moment of **6** was reported by Karlin et al. to be 4.16 μ_B, corresponding to an S = 3/2 system.[29] We attribute the change in the low spin character of **5** to high spin in **6** to the change in apical ligand from P to N. However, we note that we are unable to make a direct comparison of the electronic effect from the different apical donors since **5** and **6** exhibit different coordination geometries in their solid state structures.

Electrochemistry. Cyclic voltammetry was performed on **5** and $[Co(TPA)(CH_3CN)][BF_4]_2$. TPA was synthesized according to a literature procedure[29] and was complexed using $[Co(CH_3CN)_6][BF_4]_2$ to give $[Co(TPA)(CH_3CN)][BF_4]_2$. Complex $[Co(TPA)(CH_3CN)][BF_4]_2$ was synthesized instead

Table 1. Selected Bond Lengths (Å) and Angles (deg) for 4 and 5

$[Co(TPAMP)_2][BF_4]_2$ (**4**)		$[Co(TPAP)(CH_3CN)][BF_4]_2$ (**5**)	
Co(1)—P(1)	2.1095(6)	Co(1)—P(1)	2.1693(7)
Co(1)—P(2)	2.1175(6)	Co(1)—N(5)	2.035(2)
Co(1)—N(2)	2.1943(19)	Co(1)—N(6)	1.997(2)
Co(1)—N(4)	2.0468(18)	Co(1)—N(7)	2.094(2)
Co(1)—N(8)	2.2169(19)	Co(1)—N(8)	1.966(2)
Co(1)—N(10)	2.0935(19)	P(1)—N(1)	2.877(2)
		P-(1)—Co(1)—N(8)	176.94(7)
		N(5)—Co(1)—N(6)	151.88(9)

DOI: 10.1021/acs.inorgchem.5b02133
Inorg. Chem. 2015, 54, 11505−11510

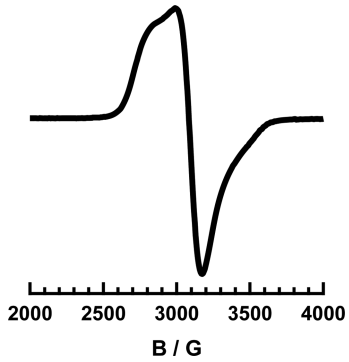

Figure 3. EPR spectrum of **5** in a frozen solution of acetonitrile at 77 K.

of the previously published complex **6** $[Co(TPA)(CH_3CN)][ClO_4]_2$ due the potential hazard of perchlorate salts.

The cyclic voltammogram of **5** in acetonitrile exhibited an irreversible oxidation event at 0.13 V and a reversible event at −1.47 V (vs $Fe(C_5H_5)_2^{0/+}$, at 100 mV/s scan rate) (Figure S9). The isolated reversible event at −1.47 V is assigned as the $Co^{+/+2}$ couple and is shown in Figure 4. Under the same

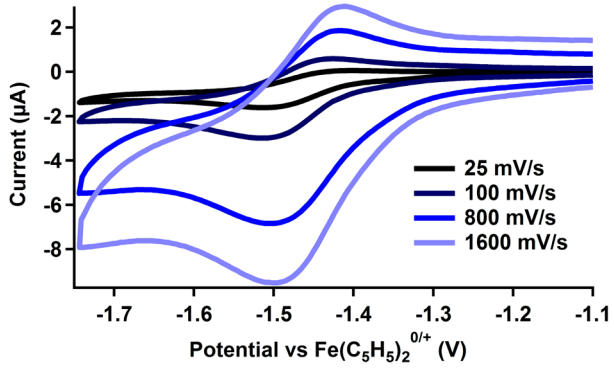

Figure 4. Variable scan rate cyclic voltammograms of **5** with 1.0 mM analyte in acetonitrile with 0.02 M Bu_4NPF_6.

conditions, $[Co(TPA)(CH_3CN)][BF_4]_2$ also exhibited an irreversible oxidation at 0.66 V (Figure S9). When isolated, the assigned $Co^{+/+2}$ couple is observed as a quasi-reversible event at −1.54 V (vs $Fe(C_5H_5)_2^{0/+}$, at 100 mV/s scan rate) (Figure S10). This reduction event matches that of other $[Co(TPA)(X)]^{2+}$ complexes reported in literature.[34]

In the study conducted by Britovsek et al. using a Ru metal center, they found that "changing the nitrogen amine donor in TPA for a strong field P-donor (and one pyridine ligand for an acetonitrile ligand) increases the $Ru^{+2/+3}$ redox potential considerably".[17] In this study, we found only a modest increase (7 mV) in the $Co^{+/+2}$ redox potential for complex **5** compared to $[Co(TPA)(CH_3CN)][BF_4]_2$.

UV−vis. The room-temperature UV−visible spectrum of **4** and **5** was obtained in acetonitrile (Figure S11 and 5, respectively). For **5**, a charge transfer band is shown in the UV region (255 nm) while two broad bands are shown in the visible region (400 and 595 nm). A fourth band is seen in the Near-IR at 975 nm. The two charge transfer bands at 255 and 400 nm have an ε value of 8064 and 3058 $M^{-1}cm^{-1}$, respectively, while the bands at 595 and 975 nm (d−d transition) have an ε value of 212 and 50.3 $M^{-1}cm^{-1}$, respectively. The latter two features are consistent with a low

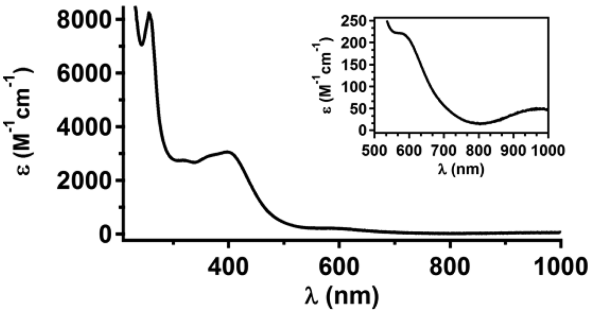

Figure 5. UV−vis spectrum of **5** in acetonitrile at 22 °C. An inset displays a close up of the bands between 500 and 1000 nm.

spin Co(II) in the coordination geometry observed in the solid state structure.

By comparison, the room-temperature UV−visible spectrum of **6** was previously reported by Karlin et al.[35] Complex **6** displayed d−d transitions at 472, 552, and 945 nm with ε value of 82, 52, and 5 $M^{-1}cm^{-1}$, respectively.

CONCLUSIONS

We have successfully modified a proazaphosphatrane to furnish the first tetradentate tripyridyl ligand featuring a phosphorus apical donor, TPAP. The magnetic properties of the $[Co(TPAP)(CH_3CN)]^{2+}$ complex displayed a different spin state (low) to that of $[Co(TPA)(CH_3CN)]^{2+}$ (high) but have similar redox properties. Comparing the coordination geometry to Co(II) for TPAMP and TPAP, which have one- and two- atom spacers between the phosphorus donor and pyridyl arms, respectively, demonstrates the importance of ligand flexibility in supporting the desired tetradentate coordination geometry. The result of our study provides a useful guide to the design of new tripodal ligands containing nonamine apical donors.

EXPERIMENTAL SECTION

General Considerations. The complexes described below are air- and moisture-sensitive, and must be handled under an inert atmosphere of nitrogen using standard glovebox and Schlenk techniques. Unless otherwise noted, all procedures were performed at ambient temperature (21−24 °C). All solvents were sparged with argon and dried using a solvent purification system. Halocarbon solvents were passed through packed columns of neutral alumina and Q5 reactant. Acetonitrile, diethyl ether, and halogenated solvents were passed through two columns of neutral alumina. Methanol was dried through columns of activated molecular sieves. Compounds tris[2-[*N*-(2-pyridinemethyl)-amino]ethyl]amine[22] (**1**), *N*,*N*′,*N*″-trimethyl-tri-(pyridylamino)phosphine (TPAMP),[17] tris(2-pyridylmethyl)amine (TPA),[29] and $[Co(CH_3CN)_6][BF_4]_2$[36] were synthesized according to established procedures. CD_3CN was freeze−pump−thawed three times and dried over molecular sieves. All other materials 2-pyridinecarboxyaldehyde (99%), tris(2-aminoethyl)amine (96%), 10% Palladium/Carbon Type 487, potassium *tert*-butoxide (97%) and bis(dimethylamino)chlorophosphine (96%) were purchased from commercial sources and used without further purification.

Physical Methods. Electrospray ionization mass spectrometry (ESI-MS) was performed with an ESI LC-TOF Micromass LCT 3 mass spectrometer. Nuclear magnetic resonance (NMR) spectra were recorded on a Bruker DRX500 spectrometer fitted with a TCI cryoprobe (^{13}C) or a DRX400 with a switchable QNP probe (^{1}H and ^{31}P) in dry, degassed solvents. ^{1}H NMR spectra were referenced to (tetramethylsilane) TMS using the residual proteo impurities of the solvent; ^{13}C NMR spectra were referenced to TMS using the natural abundance ^{13}C of the solvent; ^{31}P NMR spectra were referenced to H_3PO_4 using the Ξ scale with the corresponding ^{1}H spectra.[37] All

DOI: 10.1021/acs.inorgchem.5b02133
Inorg. Chem. 2015, 54, 11505−11510

chemical shifts are reported in the standard δ notation in parts per million; positive chemical shifts are to a higher frequency from the given reference. Elemental analyses were performed on a PerkinElmer 2400 Series II CHNS elemental analyzer. Perpendicular-mode X-band electron paramagnetic resonance (EPR) spectrum was collected using a Bruker EMX spectrometer. Electrochemical experiments were carried out on a Pine Wavedriver 10 potentiostat. Electrochemical experiments were carried out in acetonitrile solutions with 1.0 mM analyte and 0.20 M Bu_4NBF_4. The working electrode was a glassy carbon disc with a diameter of 2 mm, the counter electrode was a glassy carbon rod, and a Ag/AgCl pseudoreference electrode. Potentials were referenced to the ferrocene/ferrocenium couple at 0 V using ferrocene as an internal reference. UV−vis spectrum was collected in acetonitrile solution using an Agilent Technologies Cary 60 UV−vis.

X-ray Crystallography. X-ray diffraction studies were carried out at the UCI Department of Chemistry X-ray Crystallography Facility on a Bruker SMART APEX II diffractometer. Data were collected at 88 K for **5**, 173 K for **4** and 296 K for **2** using Mo Kα radiation (λ = 0.710 73 Å). A full sphere of data were collected for each crystal structure. The APEX2 program suite was used to determine unit-cell parameters and to collect data. The raw frame data were processed and absorption corrected using the SAINT and SADABS programs, respectively, to yield the reflection data files. Structures were solved by direct methods using SHELXS and refined against F^2 on all data by full-matrix least-squares with SHELXL-97. All non-hydrogen atoms were refined anisotropically. Hydrogen atoms other than H1 in **2** were placed at geometrically calculated positions and refined using a riding model, and their isotropic displacement parameters were fixed at 1.2 (1.5 for methyl groups) times the Ueq of the atoms to which they are bonded. H1 in **2** was located in the difference map and refined freely. For the structure of **2**, checkCIF reports three level B alerts (PLAT230_ALERT_2_B) due to unequal anisotropic displacement parameters (ADPs) along chemical bonds, which can signify an incorrect atom type assignment. However, we are confident in our assignments, as all three alerts involve bonds within a pyridine ring of the TPAP ligand whose identity has been confirmed through other spectroscopic techniques. An additional level B alert (PLAT411_ALERT_2_B) was reported for this structure due to a short nonbonding intermolecular H···H distance between two ligand hydrogen atoms (H21 and H23); this is likely a result of crystal packing. For the structure of **4**, checkCIF reports one level B alert (PLAT214_ALERT_2_B) due to a high ratio of maximum to minimum anisotropic displacement parameters (ADPs) for atom F2B, which can signify a substitutional or positional disorder. As this atom is in the minor part of a disordered BF_4 anion, the identity of which is not in question, we did not deem it appropriate to model any further disorder.

[Co(TPAMP)$_2$][BF$_4$]$_2$ ***(4)***. In the glovebox, $[Co(CH_3CN)_6][BF_4]_2$ (61.3 mg, 0.128 mmol) was added to a solution of TPAMP (45.1 mg, 0.128 mmol) in 3 mL of dichloromethane. The solution immediately turned dark green and was stirred for 6 h at room temperature. The solvent was removed under reduced pressure, and the resulting green solid was washed with diethyl ether. The green solid was redissolved in acetonitrile and filtered through a glass pipet packed with a glass microfiber filter. Slow vapor diffusion with diethyl ether afforded green crystals. ESI-MS (m/z): $[M - BF_4]^+$ Calculation for $C_{36}H_{42}BCoF_4N_{12}P_2$, 850.25; Found, 850.17. UV−vis (CH_3CN) λ_{max}, nm (ε): 230 (49377), and 290 (18654). Analytical Calculation for $C_{36}H_{42}B_2Cl_3CoF_8N_{12}P_2\cdot(CH_2Cl_2)_{1.5}$: C, 42.14; H, 4.13; N, 15.92. Found: C, 42.30; H, 4.26; N, 15.79. μ_{eff} (solution) = 2.11 μ_B.

[HP((2-PyrCH$_2$)-NCH$_2$CH$_2$)$_3$N][Cl] ([HTPAP][Cl]) ***(2)***. In the glovebox, a solution of **1** (200 mg, 0.476 mmol) in 5 mL of tetrahydrofuran was added to a solution of bis(dimethylamino)chlorophosphine (111 mg, 0.715 mmol) in 10 mL of tetrahydrofuran. The mixture was stirred overnight, at which time a white solid precipitated out of solution. The solution was filtered through a medium fritted funnel, and the precipitate was washed with tetrahydrofuran and dried on the high vacuum line to afford a white solid in 61.9% yield. ^{1}H NMR (CD_3CN, 400 MHz) δ = 3.16 (m, 6H, $PNCH_2CH_2N$), 3.25 (m, 6H, $PNCH_2CH_2N$), 4.25 (d, J = 19.1 Hz, 6H, $PyrCH_2N$), 5.84 (d, J = 506 Hz, 1H, P-*H*), 7.23 (m, 3H, Pyr), 7.28 (d, J = 7.8 Hz, 3H, Pyr), 7.70 (td, J = 7.7, 1.9 Hz, 3H, Pyr), 8.51 (d, J = 5.5 Hz, 3H, Pyr). $^{13}C\{^1H\}$NMR (CD_3CN, 126 MHz) δ = 40.25 (NCH_2CH_2NP), 47.91 ($PhCH_2N$), 53.39 (NCH_2CH_2NP), 122.6 (Pyr), 123.4 (Pyr), 137.87 (Pyr), 150.5 (Pyr), 159.2 (Pyr). $^{31}P\{^1H\}$NMR (CD_3CN, 162 MHz) δ = −10.00. ^{31}P NMR (CD_3CN, 162 MHz) δ = −10.00 (d, $^1J_{P-H}$ = 506 Hz). ESI-MS (m/z): $[M - Cl]^+$ Calculation for $C_{24}H_{31}N_7P$, 448.27; Found, 448.23.

P((2-PyrCH$_2$)-NCH$_2$CH$_2$)$_3$N (TPAP) ***(3)***. In the glovebox, a solution of potassium *tert*-butoxide (148 mg, 1.32 mmol) in 5 mL of tetrahydrofuran was added to a suspension of [HTPAP][Cl] (320 mg, 0.661 mmol) in 10 mL of tetrahydrofuran. The mixture was stirred overnight and KCl precipitated from the solution. The reaction was filtered through a medium fritted funnel. The filtrate was collected, and the solvent was removed under reduced pressure. The solid was redissolved in acetonitrile and refiltered through a medium fritted funnel to remove excess potassium *tert*-butoxide. The filtrate was collected, the solvent was removed under reduced pressure, and the solid was redissolved in tetrahydrofuran and layered with pentane. After 1 day of standing, the solution was decanted from crystalline KCl and potassium *tert*-butoxide. The solvent from the filtrate was removed under reduced pressure to afford the product as a tan solid in 85.4% yield. ^{1}H NMR (CD_3CN, 400 MHz) δ = 2.76 (m, 6H, $PNCH_2CH_2N$), 2.84 (m, 6H, $PNCH_2CH_2N$), 4.29 (d, J = 10.8 Hz, 6H, $PyrCH_2N$), 7.19 (m, 3H, Pyr), 7.47 (m, 3H, Pyr), 7.71 (td, J = 7.6, 1.8 Hz, 3H, Pyr), 8.49 (m, 3H, Pyr). $^{13}C\{^1H\}$NMR (CD_3CN, 126 MHz) δ = 47.2 (NCH_2CH_2NP), 51.7 ($PyrCH_2N$), 55.8 (NCH_2CH_2NP), 122.8 (Pyr), 122.9 (Pyr), 137.5 (Pyr), 150.0 (Pyr), 162.5 (Pyr). $^{31}P\{^1H\}$NMR (CD_3CN, 162 MHz) δ = 126.6. ESI-MS (m/z): $[M + H]^+$ Calculation for $C_{24}H_{31}N_7P$, 448.27; Found, 448.27.

[Co(TPAP)(CH$_3$CN)][BF$_4$]$_2$ ***(5)***. In the glovebox, $[Co(CH_3CN)_6][BF_4]_2$ (23.8 mg, 0.049 mmol) was added to a solution of TPAP (22.2 mg, 0.049 mmol) in 3 mL of acetonitrile. The solution immediately turned dark greenish brown and was stirred for 6 h at room temperature. The solvent was removed under reduced pressure, and the resulting green solid was washed with diethyl ether. The green solid was redissolved in dichloromethane and filtered through a glass pipet packed with a glass microfiber filter. To this solution, diethyl ether was layered to afford green crystals that were isolated in 56.2% yield. ESI-MS (m/z): $[M - BF_4 - CH_3CN]^+$ Calculation for $C_{24}H_{30}BCoF_4N_7P$, 593.17; Found, 593.17. UV−vis (CH_3CN) λ_{max}, nm (ε): 255 (8064), 400 (3058), 595 (212) and 975 (50.3). Analytical Calculation for $C_{26}H_{33}B_2CoF_8N_8P$: C, 43.31; H, 4.61; N, 15.54. Found: C, 42.64; H, 4.58; N, 15.01. μ_{eff} (solution) = 2.67 μ_B.

[Co(TPA)(CH$_3$CN)][BF$_4$]$_2$. In the glovebox, $[Co(CH_3CN)_6][BF_4]_2$ (100 mg, 0.209 mmol) was added to a solution of TPA (60.6 mg, 0.209 mmol) in 5 mL of acetonitrile. The solution became purple and was stirred for 1 h at room temperature. The solvent was removed under reduced pressure, and the resulting purple solid was washed with diethyl ether. The purple solid was redissolved in acetone and filtered through a glass pipet packed with a glass microfiber filter. To this solution, diethyl ether was layered to grow purple crystals that were isolated in 87.7% yield. ESI-MS (m/z): $[M - (BF_4)_2 - CH_3CN]^{2+}$ Calculation for $C_{18}H_{18}CoN_4$, 174.54; Found, 175.51. Analytical Calculation for $C_{20}H_{21}B_2CoF_8N_5\cdot(C_3H_6O)_{0.75}$: C, 43.99; H, 4.23; N, 11.53. Found: C, 43.52; H, 4.11; N, 11.02.

■ ASSOCIATED CONTENT

Supporting Information

The Supporting Information is available free of charge on the ACS Publications website at DOI: 10.1021/acs.inorgchem.5b02133.

CIF files (CCDC deposition numbers) for **4** (1409177), **2** (1420592), and **5** (1409176). ^{1}H, $^{13}C\{^1H\}$, $^{31}P\{^1H\}$ NMR data for **2** and **3**, magnetic susceptibility data, cyclic voltammograms, UV−vis spectrum, and compiled structural data and analysis of previously published

DOI: 10.1021/acs.inorgchem.5b02133
Inorg. Chem. 2015, 54, 11505−11510

Verkade's superbase (Table S1) and Co(II) TPA and TEPA complexes (Table S2 and S3). (PDF)
X-ray crystal data and tables for **4** (Tables S9−S13) (CIF)
X-ray crystal data and tables for **2** (Tables 14−S18) (CIF)
X-ray crystal data and tables for **5** (Tables S4−S8) (CIF)

AUTHOR INFORMATION

Corresponding Author

*E-mail: j.yang@uci.edu (J.Y.).

Notes

The authors declare no competing financial interest.

ACKNOWLEDGMENTS

The authors would like to thank Prof. A. S. Borovik for helpful discussions. The authors would also like to thank Nathaniel Lau for assistance with the TOC and Dr. Joseph W. Ziller for X-ray support. This material is based upon work supported by the U.S. Department of Energy, Office of Science, Office of Basic Energy Sciences under Award Number DE-SC0012150.

REFERENCES

(1) Blackman, A. G. *Eur. J. Inorg. Chem.* **2008**, *17*, 2633−2647.
(2) Kakuda, S.; Peterson, R. L.; Ohkubo, K.; Karlin, K. D.; Fukuzumi, S. *J. Am. Chem. Soc.* **2013**, *135*, 6513−6522.
(3) Morimoto, Y.; Bunno, S.; Fujieda, N.; Sugimoto, H.; Itoh, S. *J. Am. Chem. Soc.* **2015**, *137*, 5867−5870.
(4) Oloo, W. N.; Meier, K. K.; Wang, Y.; Shaik, S.; Münck, E.; Que, L. *Nat. Commun.* **2014**, *5*, 3046.
(5) Klotz, K. L.; Slominski, L. M.; Hull, A. V.; Gottsacker, V. M.; Mas-Balleste, R.; Que, J. L.; Halfen, J. A. *Chem. Commun.* **2007**, *20*, 2063−2065.
(6) Kaur, A.; Ribelli, T. G.; Schröder, K.; Matyjaszewski, K.; Pintauer, T. *Inorg. Chem.* **2015**, *54*, 1474−1486.
(7) Lewis, E. A.; Tolman, W. B. *Chem. Rev.* **2004**, *104*, 1047−1076.
(8) Min, K. S.; DiPasquale, A. G.; Rheingold, A. L.; White, H. S.; Miller, J. S. *J. Am. Chem. Soc.* **2009**, *131*, 6229−6236.
(9) Shin, D. M.; Lee, I. S.; Lee, Y.-A.; Chung, Y. K. *Inorg. Chem.* **2003**, *42*, 2977−2982.
(10) Manzur, J.; Musker, W. K. *Inorg. Nucl. Chem. Lett.* **1973**, *9*, 841−843.
(11) Leung, W.-P.; Weng, L.-H.; Kwok, W.-H.; Zhou, Z.-Y.; Zhang, Z.-Y.; Mak, T. C. W. *Organometallics* **1999**, *18*, 1482−1485.
(12) de la Lande, A.; Gérard, H.; Moliner, V.; Izzet, G.; Reinaud, O.; Parisel, O. *JBIC, J. Biol. Inorg. Chem.* **2006**, *11*, 593−608.
(13) Over, D.; de la Lande, A.; Zeng, X.; Parisel, O.; Reinaud, O. *Inorg. Chem.* **2009**, *48*, 4317−4330.
(14) Schenk, S.; Reiher, M. *Inorg. Chem.* **2009**, *48*, 1638−1648.
(15) Hölscher, M.; Leitner, W. *Eur. J. Inorg. Chem.* **2006**, *21*, 4407−4417.
(16) Chiswell, B. *Aust. J. Chem.* **1967**, *20*, 2533−2534.
(17) Whiteoak, C. J.; Nobbs, J. D.; Kiryushchenkov, E.; Pagano, S.; White, A. J. P.; Britovsek, G. J. P. *Inorg. Chem.* **2013**, *52*, 7000−7009.
(18) Batke, S.; Sietzen, M.; Wadepohl, H.; Ballmann, J. *Inorg. Chem.* **2014**, *53*, 4144−4153.
(19) Sietzen, M.; Batke, S.; Merz, L.; Wadepohl, H.; Ballmann, J. *Organometallics* **2015**, *34*, 1118−1128.
(20) Verkade, J. G.; Kisanga, P. B. *Tetrahedron* **2003**, *59*, 7819−7858.
(21) Kisanga, P. B.; Verkade, J. G. *Tetrahedron* **2001**, *57*, 467−475.
(22) Deroche, A.; Morgenstern-Badarau, I.; Cesario, M.; Guilhem, J.; Keita, B.; Nadjo, L.; Houée-Levin, C. *J. Am. Chem. Soc.* **1996**, *118*, 4567−4573.
(23) Laramay, M. A. H.; Verkade, J. G. *J. Am. Chem. Soc.* **1990**, *112*, 9421−9422.
(24) Lensink, C.; Xi, S. K.; Daniels, L. M.; Verkade, J. G. *J. Am. Chem. Soc.* **1989**, *111*, 3478−3479.
(25) Chatelet, B.; Gornitzka, H.; Dufaud, V.; Jeanneau, E.; Dutasta, J.-P.; Martinez, A. *J. Am. Chem. Soc.* **2013**, *135*, 18659−18664.
(26) Kisanga, P. B.; Verkade, J. G.; Schwesinger, R. *J. Org. Chem.* **2000**, *65*, 5431−5432.
(27) Verkade, J. G. *Acc. Chem. Res.* **1993**, *26*, 483−489.
(28) Addison, A. W.; Rao, T. N.; Reedijk, J.; van Rijn, J.; Verschoor, G. C. *J. Chem. Soc., Dalton Trans.* **1984**, *7*, 1349−1356.
(29) Nanthakumar, A.; Fox, S.; Murthy, N. N.; Karlin, K. D. *J. Am. Chem. Soc.* **1997**, *119*, 3898−3906.
(30) Xi, S. K.; Schmidt, H.; Lensink, C.; Kim, S.; Wintergrass, D.; Daniels, L. M.; Jacobson, R. A.; Verkade, J. G. *Inorg. Chem.* **1990**, *29*, 2214−2220.
(31) Tang, J. S.; Laramay, M. A. H.; Young, V.; Ringrose, S.; Jacobson, R. A.; Verkade, J. G. *J. Am. Chem. Soc.* **1992**, *114*, 3129−3131.
(32) Benelli, C.; Di Vaira, M.; Noccioli, G.; Sacconi, L. *Inorg. Chem.* **1977**, *16*, 182−187.
(33) Rupp, R.; Huttner, G.; Kircher, P.; Soltek, R.; Büchner, M. *Eur. J. Inorg. Chem.* **2000**, *2000*, 1745−1757.
(34) Ward, A. L.; Elbaz, L.; Kerr, J. B.; Arnold, J. *Inorg. Chem.* **2012**, *51*, 4694−4706.
(35) Chufán, E. E.; Verani, C. N.; Puiu, S. C.; Rentschler, E.; Schatzschneider, U.; Incarvito, C.; Rheingold, A. L.; Karlin, K. D. *Inorg. Chem.* **2007**, *46*, 3017−3026.
(36) Useful Reagents and Ligands. In *Inorganic Syntheses*; John Wiley & Sons, Inc.: 2002; pp 75−121.
(37) Harris, R. K.; Becker, E. D.; Cabral de Menezes, S. M.; Goodfellow, R.; Granger, P. *Pure Appl. Chem.* **2001**, *73*, 1795−1818.

DOI: 10.1021/acs.inorgchem.5b02133
Inorg. Chem. 2015, 54, 11505−11510